Hardware Implementation of Underwater Acoustic Localization System for Bridge Scour Monitoring

Yahong Rosa Zheng[1], Zengli Yang[1], Jinxing Hao[2], Peng Han[3]

[1]Dept. of Electrical & Computer Engineering, Missouri University of Science & Technology, Rolla, MO 65409
[2]Department of Electronic Engineering, Tsinghua University, Beijing 100084, China
[3]College of Marine Engineering, Northwestern Polytechnical University, Xi'an, 710072, China

***Abstract*—This paper reports the first round of design and hardware implementation experience for localization of acoustic transmitter in a river. The application of the acoustic localization is bridge scour monitoring where smart rocks are equipped with acoustic communication systems to communicate with nodes at river banks. The time difference of arrival (TDOA) is measured by transmitting maximum-length pseudo-noise (PN) sequences and payload periodically using On-Off Keying (OOK) modulation at carrier frequency of 125 kHz. The receiver nodes at river banks use simple non-coherent detection to find the peak of PN correlation. The detected peak indexes are then used to estimate the TDOA for localizing the transmitter. The hardware transceiver is implemented on a Texas Instruments (TI) digital signal processor (DSP) platform. The major challenges encountered in the implementation and field tests included timing errors at separate transceivers, transceiver front end for high carrier frequency, environmental harshness, electro-magnetic interference, and acoustic multi-paths. Remedies are reported, including using GPS receivers at riverbank nodes, bandpass sampling and interface of ADC/DAC to DSP, and first-arrival peak detection algorithm.**

I. Introduction

The major cause of bridge collapses in the U.S. is due to the scour [1]. However, scour monitoring is conventionally performed by divers or robot cameras which can be very costly and unsafe, especially during stormy or flooding seasons. A smart rock concept has been proposed to equip manmade rocks with Radio Frequency (RF) communication means or acoustic communication transceivers so that, when placed together with natural rocks under the bridge, the locations of the smart rocks are estimated through the communication signals between the smart rocks and the gateway nodes near the river bank. As shown in Fig. 1, the gateway nodes can relay the localization data via cellular networks to headquarter of the monitoring system and scour monitoring can be performed with low risk and at realtime even during rain storms.

In contrast to source localization using RF signal strength indicator (RSSI), acoustic communication waves propagates at a low speed and the Time of Arrival (TOA) or Time Difference of Arrival (TDOA) [2] can be employed to estimate the short distances between the transmitter in the smart rock and the receivers at gateway nodes. When many smart rocks are placed near river piers, temporal and spatial information of scour process can be monitored and when significant displacement of smart rocks occurs, the scour information can be used for early warning and early repair guide.

Utilizing TDOA for localization has some advantages over RSSI in the smart rocks application because the TDOA can be estimated with better reliability than the RSSI due to the short distances between the rocks and gateway nodes. However, commercial underwater acoustic communications systems are not only expensive, but also inflexible to adapt to this application. This motivates us to design and implement our own hardware for underwater acoustic (UWA) communications system for smart rocks.

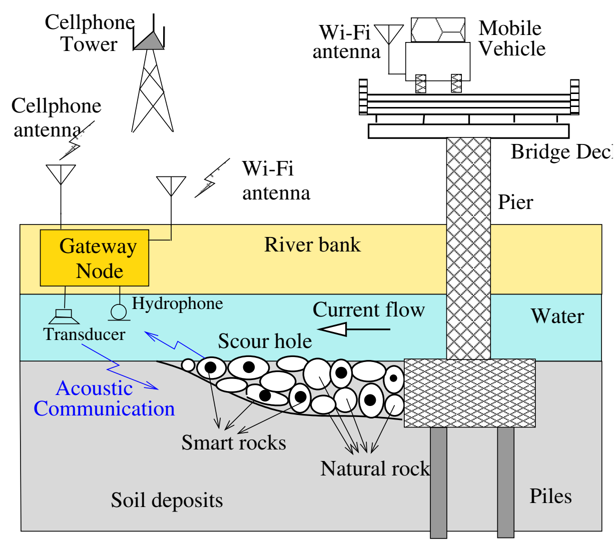

Fig. 1. Smart rocks for bridge scour monitoring.

We identify three main challenges in UWA localization of smart rocks: one is the multipath propagation [3] [4] that can result in stronger late arrivals than the direct line of sight path. This challenge is similar to the RF wave propagation and localization [6]. The second is the timing synchronization among multiple gate node receivers, as multiple receiver platforms are placed at two sides of the river, as shown in Fig. 2. The third one is timing calibration of the localization signals at the transmitters. In this paper, we address these issues on the hardware design based on the Texas Instruments (TI) Digital Signal Processor (DSP) platform TMS320C6713.

978-0-933957-40-4 ©2013 MTS

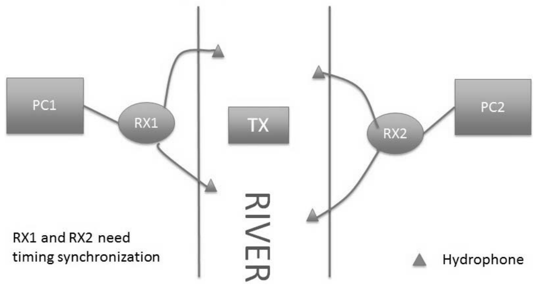

Fig. 2. Placement of smart rock transmitter and receivers in a river.

II. The Proposed TDOA Detection Approach

The proposed acoustic communication system is shown in Fig. 3, where transmitter first encodes the information bits and combines one or two preamble sequences before modulating to carrier frequency with On-Off Keying (OOK). Zeros (gaps) are then padded to form N bits per block. An DAC (digital to analog convertor) is used to convert digitally modulated signals to analog signals. Power amplifier and load matching network are used to tune the signal output to the acoustic projector.

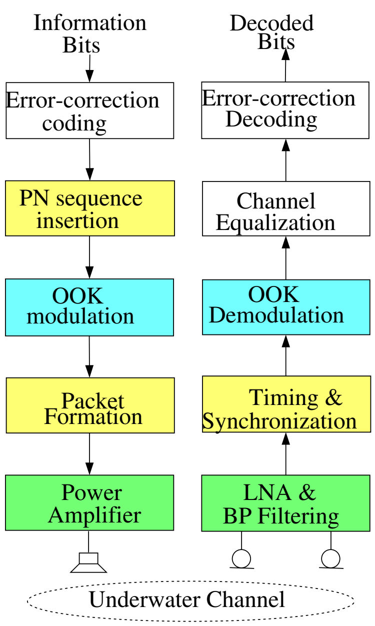

Fig. 3. Acoustic transceiver block diagram.

The transmitted data frame structure is shown in Fig. 4. We used two block structures, both had $N = 250$ bits per block with a bit rate of $R = 5000$ bps. Design 1 had $N_1 = 63$ bits preamble of maximum length PN sequence, no preamble 2 or $N_2 = 0$, payload length $N_3 = 16$ bits, and $N_4 = 171$ padded zeros. Design 2 used two identical preambles $N_1 = N_2 = 64$ which was a 63-bit m-sequence plus a padded one, a payload of $N_3 = 15$ bits, and $N_4 = 107$ padded zeros.

The receiver utilizes a bandpass filter and a low-noise amplifier to filter the desired signals into the digital receiver. Analog to Digital Convertors (ADC) are used to convert the zero IF

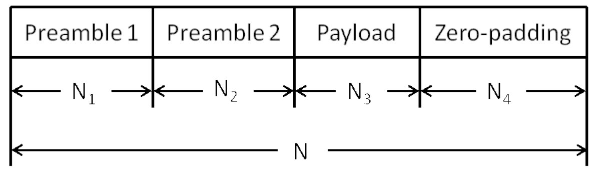

Fig. 4. Transmitted signal frame structure for localization.

signals directly to digital signal and a simple non-coherent rectifier is used to demodulate the OOK signal to baseband symbols. Timing and bit synchronization are then estimated by correlating the PN sequence with the demodulated signal and peak detection is used to estimate the block start indexes. If multipaths are strong, channel estimation and equalization are used to reduce the intersymbol interference (ISI) and then bit detection follows the channel decoding.

The transmitter hardware consists of the TI TMS320C6713 starter board, an Analog Devices 12-bit DAC, a power amplifier and matching network (BII), and an acoustic projector (BTech 1201). The data blocks are transmitted repeatedly for localization purposes with payload bits changing block by block. The on-off keying (OOK) modulation were implemented in the DSP, where bit 1 is represented by a memory bank of pre-computed cosine wave of frequency $f_c = 125$ kHz at a sampling rate of 3 MHz, and bit 0 is represented by DC voltage. The QDMA memory transfer [9] is used to send the modulated OOK signals to the DAC. The receiver consists of two channels of hydrophones, analog bandpass filters, low-noise amplifiers (LNA), and analog to digital converters (ADC). The two 12-bit ADC channels are interfaced with one C6713 board via the external memory interface (EMIF). The sampling rate at the receiver was 55 kHz to yield a bandpass sampling carrier at 15 kHz and 11 samples per bit. Fig. 5 shows the hardware diagram of the acoustic receiver on DSP.

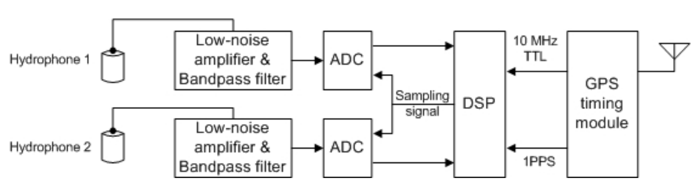

Fig. 5. Receiver structure based on DSP.

When multiple DSP receivers with multiple channels are required for field deployment, for example, at both sides of a river, timing synchronization among the receivers is critical to the TDOA localization method. Several options for the timing synchronization of multiple receivers have been researched and simulated. We chose a commercial GPS timing module and integrated it into each DSP receiver. The GPS timing module provides the one pulse per second (1PPS) signal to the DSPs of the receivers that are placed at different locations. Therefore, sampling and recording of all the hydrophones at all the receivers are synchronized by the 1PPS reference.

Fig. 6 shows the hardware setup for the timing synchronization. The 1PPS signal from the GPS timing module triggers the DSP as the external interrupt, then the DSP generates the 55 kHz sampling signals for the ADCs. This method can mitigate the effect of difference of the sampling frequencies between the transmitter and multiple receivers because the frequency accuracy of the ovenized piezo-electrical crystal oscillators used on the DSP boards is at around 5 – 10 PPM (part per million) which results in a drift of one to two samples in every two seconds of the transmitted signals. This accuracy is not enough for accurate long-term timing estimation. We used the calibration procedure to reduce the drft at the transmitter side. In the receivers, data inputs and recording have to be synchronized too. With the aid of GPS, the accuracy improves to 0.5 PPM.

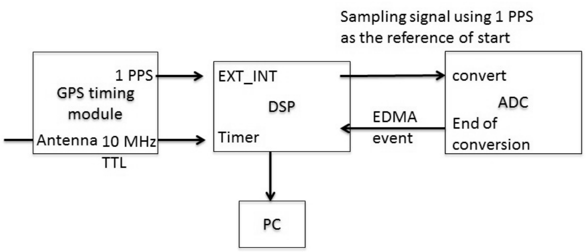

Fig. 6. GPS interfaces with DSP.

By measuring the time indexes of the correlation peaks from different hydrophones, we are able to obtain their TDOAs. With the TDOA information, we can implement the efficient localization algorithms such as the one in [6], [7]. Note that the acoustic wave propagates at different speed at different water temperature. According to the empirical formula [8]

$$\begin{aligned} c \;=\; & 1.40238742 \times 10^{3} + 5.038821344T \\ & -5.80539349 \times 10^{-2}T^{2} + 3.32000870 \times 10^{-4}T^{3} \\ & -1.44537900 \times 10^{-6}T^{4} + 2.99402365 \times 10^{-9}T^{5} \quad \text{(m/s)} \end{aligned}$$

where T is the water temperature in Celsius. For example, at temperature of $T = 5°$C, the speed of sound in water is calculated as $c = 1426$ m/s, and the range resolution is 0.2852 m/bit. With upsampling of $D = 11$ samples per bit, the range resolution is 0.026 m/sample.

III. Laboratory and Field Tests

A. TDOA Estimation in Laboratory Test

Indoor laboratory tests were conducted by lining the transmit signals directly to receiver inputs without power amplifier and low noise amplifiers. The tests identified timing drift of the transmitter, as shown in Fig. 7. Both receive channels show a drift of 45 samples (at $F_s = 55$ kHz) per 19 seconds. The ovenized oscillator on the TI DSP board had an accuracy of 5–10 PPM which matched the amount of drift measured in the tests. The timing drift was then corrected by adjusting the length of the last transmitted bit of each block through transmitter C++ programs. The resulting timing drift after the calibration was reduced to 1 sample in 20 second.

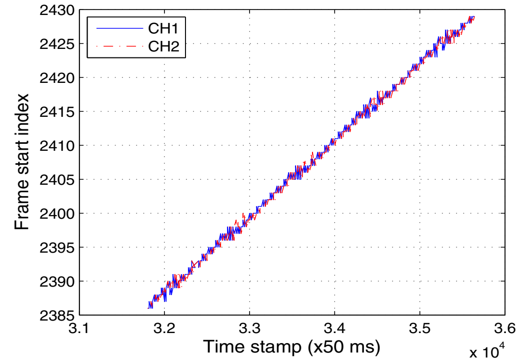

Fig. 7. laboratory test results demonstrate peak index drift due to inaccurate timing at the transmitter.

B. TDOA Estimation in Field Tests

Field Test 1:

The underwater acoustic localization experiments using one receiver were conducted in a pond at the Rolla Lions Club Park, Rolla, MO, in March 2013. The pond and its wooden deck are shown in Fig 8(a). The relative locations of the projector and hydrophones are shown in Fig. 8(b). The transmission distances ranged from 2 meters to 30 meters. Signal reception was pretty good with SNR over 20 dB.

(a) Experiment was performed near the deck as marked.

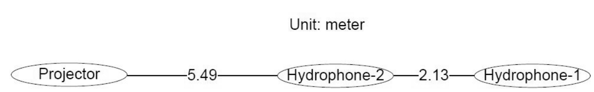

(b) Relative locations of the projector and hydrophones.

Fig. 8. Experiment setup for Field Test 1 in a pond at the Rolla Lions Club Park, Rolla, MO.

The C6713 DSP at the receiver processed the 2-channel signals simultaneously and calculated the distance difference and bit error rate (BER). Typical received passband signals at the two hydrophones are shown in Fig. 9. Two major propagation paths can be clearly identified in these signals.

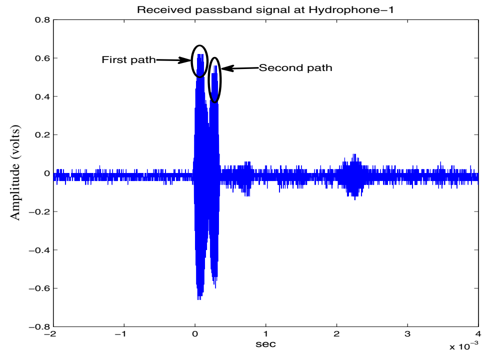

(a) Receiver 1

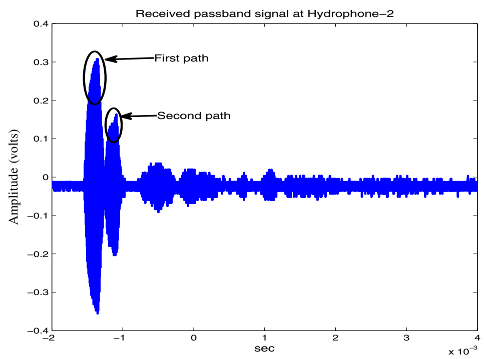

(b) Receiver 2

Fig. 9. The received passband signals at the two hydrophones when transmitting the 63-bits maximum-length PN-sequence and 8 payload bits.

However, the first arrival was always stronger. Therefore, by simple cross-correlation between the received signal and the PN sequence, the first-arriving peak was detected for each channel and their indexes were recorded. Their TDOA shows that the mean distance difference between the two hydrophones was estimated as 2.18 m with multiple trials. The estimation error between the acoustic measurement and the ground truth was 0.05 m.

Field Test 2:

Three field tests were conducted in May 2013 at a small wooden bridge on Pine Lake, near Pine Forest Drive, Rolla, MO. The area and the lake are shown in Fig. 10, where the wooden bridge runs across the island and the side of the lake. We placed two receivers, each having two hydrophones, at two ends of the wooden bridge. We denote the two channels of the first receiver (Rx1) as Ch1 and Ch2, and the two channels of the second receiver (Rx2) as Ch3 and Ch4.

The relative locations of the projector (transmitter) and hydrophones (receivers) are marked as 1 - 7 in Fig. 10, whose true locations were measured by a Total Station, as shown in Table 1. Similar locations were used in the other two experiments. The transmitter at locations 5 - 7 was transmitted one at a time. Altogether, 16 trials were conducted, each collects data for 2 to 5 minutes.

The signals received at all channels were very noisy and

Fig. 10. Experiment spot for Field Test 2 at Pine Lake, Rolla, MO.

TABLE I
TRUE LOCATIONS OF TX AND RXS IN FIELD TEST 2 AT PINE LAKE

Points	(x,y) coordinates(ft)	Tx/Rx	Transducer type
1	$(-42.829, 36.725)$	Rx1 ch1	BII Hydrophone
2	$(-56.475, -32.045)$	Rx1 ch2	BII Hydrophone
3	$(-6.596, 40.353)$	Rx2 ch3	BTech Transducer
4	$(-12.120, -44.261)$	Rx2 ch4	BTech Transducer
5	$(-26.755, 11.860)$	Tx	BTech Transducer
6	$(-22.687, 7.408)$	Tx	BTech Transducer
7	$(-27.569, 8.090)$	Tx	BTech Transducer

contained very long and strong multi-paths. The multi-path delay spread was as large as 40 — 50 bits long. The TDOA was estimated by correlating the received pass-band signals with the upsampled 63-bit PN sequence and detecting the correlation peak. The sample index corresponding to the peak is considered the first arrival of the PN sequence, as shown in Fig. 11. The two examples show the frame start index detected in Trial 16. Since simple rectifier was used for demodulation, the correlation output, shown as the red curve in both subfigures, are very spiky. Therefore, a left sliding window and a right sliding window were used to average the correlation output. The averaged correlation curves were proportional to the energy of the signal in the windows, as shown as the green and blue curves in both figure. By comparing the amplitudes of the two curves, the energy of the OOK PN sequence can be detected, within which the peak index was searched and the index corresponding to the maximum peak was taken as the frame start index. The detected indexes are used to compute the TDOA for locating the transmitter.

Three challenges were encountered in the experiments: First, two peaks may present in each acquisition of the two channels per receiver, as shown in Fig. 11(b); Second, multipath echoes may cause large estimation errors because later arrivals maybe stronger than the first arrival, as shown in Fig. 12; Third, sampling frequencies between transmitter and receivers may drift, causing estimation drifts due to the loss of GPS synchronization. For example, Fig. 13 shows that Ch3 and Ch4 experienced significant index drift that we think was mainly caused by the inaccurate 1PPS signals. Sometimes Ch1 missed the peaks due to low SNR.

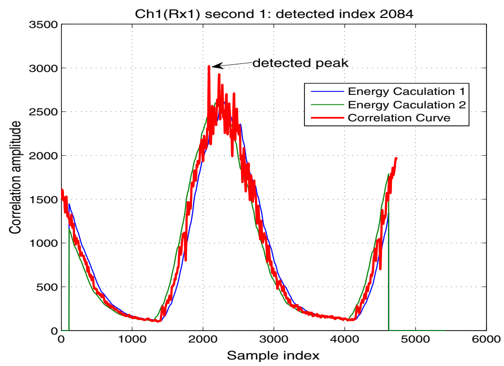

(a) Good detection: Ch 1, Second 1, Trial 16

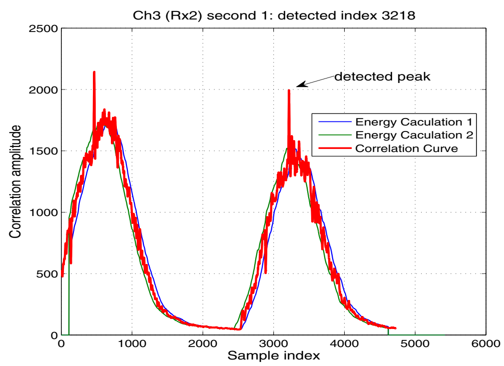

(b) Good detection: Ch 3, Second 1, Trial 16

Fig. 11. Good frame start index detection Examples.

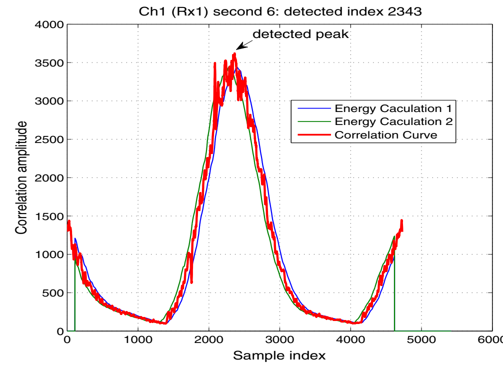

(a) Bad detection: Ch 1, Second 6, Trial 16

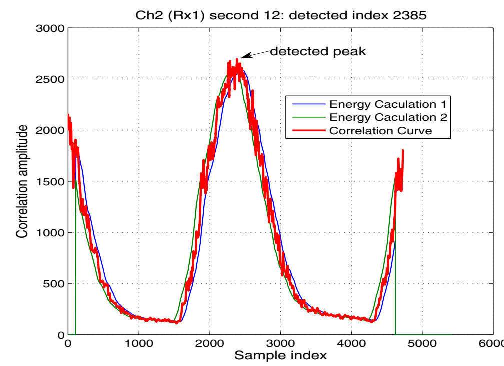

(b) Bad detection: Ch 2, Second 12, Trial 16

Fig. 12. Bad frame start index detection Examples.

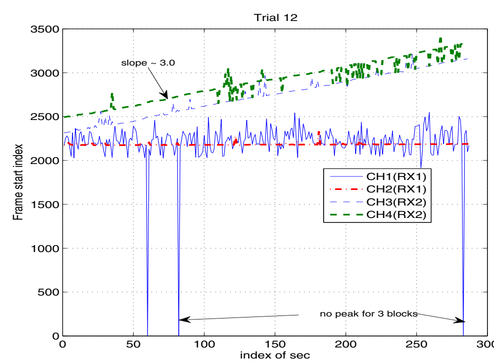

Fig. 13. Detection of frame start index in Trial 12, Field Test 2.

Observations from these figures can draw some insights into the current peak detection scheme: First, the estimated peak indexes in receiver1 tend to be larger than the true indexes, mainly due to the strong multipath echoes that added constructively at a later arrival time; Second, when the peak detection experience large errors, the bit detection also experiences large BER and good BER performance also corresponds to good peak detection. However, accurate peak detection may not guarantee good BER performance.

Field Test 3:

After mitigating the frequency drift at the transmitter side, the third field test was conducted in July, 2013 in Roubidoux Creek, Waynesville, MO. The surveyed locations of the transmitter and the receivers are listed in Table II. The locations of the transducers and the area map are shown in Fig. 14. All transmitter and receivers used BTech transducers.

TABLE II
TRUE LOCATIONS OF TX AND RXS IN FIELD TEST 3 AT ROUBIDOUX CREEK BRIDGE

Tx/Rx	(x,y) coordinates(ft)	Distance to Tx(ft)
Rx1 ch1 (point 2)	$(-20.234, -86.326)$	22.0366
Rx1 ch2 (point 1)	$(-38.907, -117.217)$	20.1167
Rx2 ch3 (point 3)	$(01.740, -97.297)$	25.1491
Rx2 ch4 (point 4)	$(-9.934, -134.406)$	28.2457
Tx (point 5)	$(-20.848, -108.354)$	

Receiver pass-band signals of ten trials were collected, each lasted for 1 to 2 minutes. The data shows better SNR than those recorded in Field Test 2 but lower SNR than those in Field Test 1. Typical peak detection performance is shown in Fig. 15(a), where the frame start index was well detected, except for the first five blocks due to data recording time needed in the hardware setup. A few intermediate blocks also experience mal-detection due to strong interference or low SNR. The BER of the unequalized PN sequence is shown in Fig. 15(b). To improve the robustness of the average TDOA estimation, the blocks whose raw BER were under a certain level, say 0.2 or 0.3, were selected to calculate the TDOA

Fig. 14. Experiment spot for Field Test 3 at I-44 Roubidoux Creek Bridge, Waynesville, MO.

and distance difference between channels; while the blocks with high BER were removed from the average. With the measured water temperature being $T = 29°$C, the estimated range differences between the channels are listed in Table III.

TABLE III
MEASURED RX-TX RANGE DIFFERENCES IN FIELD TEST 3

Rx-Tx ranges	ground truth	measured mean	variance
Ch1-Tx and Ch2-Tx	0.5852 m	0.6177 m	$0.000736m^2$
Ch1-Tx and Ch3-Tx	−0.9486 m	−1.3053 m	$0.0019m^2$
Ch3-Tx and Ch4-Tx	−0.9438 m	−0.8236 m	$0.0065m^2$

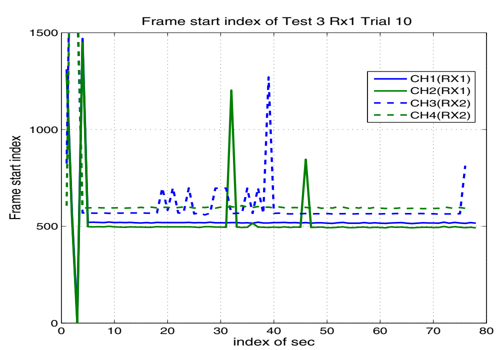

(a) Detection of frame start index

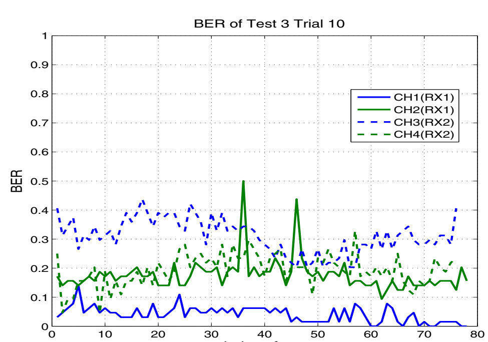

(b) Raw BER of uncoded PN sequences

Fig. 15. Performance of Trial 10, Field Test 3.

IV. CONCLUSION

The hardware of underwater acoustic localization system for bridge scour monitoring has been presented, which employs GPS receivers for timing synchronization, ADC and DAC for data reception and transmission, TI DSP for digital processing. Several tests have been conducted in laboratory and fields. Results demonstrated several challenges in achieving accurate timing and TDOA estimation and our remedies to these problems have demonstrated satisfactory results. In strong multipath acoustic channels, robust algorithms for PN sequence correlation peak detection can be further improved.

ACKNOWLEDGMENTS

Financial support for this study was provided by the U.S. Department of Transportation Research and Innovative Technology Administration (USDOT/RITA) under Cooperative Agreement No.RITARS-11-H-MST with Mr. Caesar Singh as Program Manager. In addition, Missouri Department of Transportation provided in-kind match funds for the completion of this study. The views, opinions, findings and conclusions reflected in this paper are the responsibility of the authors only and do not represent the official policy or position of the USDOT/RITA or any State or other entity. We acknowledge the help provided by other researchers in the project team: Dr. Genda Chen, Dr. David Pommerenke, Mr. Brandon P. Schafer, and Mr. Andriy Radchenko. We also thank Mr. Bing Han for helping with the field experiments and Mr. David Hoffman for surveying the true locations of the transmitter and receivers in the field experiments.

REFERENCES

[1] L. B. Becker, "Investigation of bridge scour at selected sites on Missouri streams," *U.S. Geological Survey Water-Resources Investigations Report*, 94-4200, 1994, 40 p.

[2] L. Yang, and K. C. Ho, "An approximately efficient TDOA localization algorithm in closed-form multiple disjoint sources with erroneous sensor positions," *IEEE Trans. Signal Process*, vol. 57, no. 12, pp. 4598–4615, Dec. 2009.

[3] M. Stojanovic, and J. Preisig, "Underwater acoustic communication channels: propagation models and statistical characterization," *IEEE Comm. Mag.*, vol. 47, no. 1, pp. 84–89, Jan. 2009.

[4] V. Chandrasekhar, W.K. Seah, Y. S. Choo, and H. V. Ee, "Localization in underwater networks - survey and challenges," *ACM Int'l Conf. Mobile Computing and Networking (MobiCom)*, New York, NY, USA, Sep. 2006, pp. 33–40.

[5] H. Yan, L. Wan, S. Zhou, Z. Shi, J. Cui, J. Huang, and H. Zhou "DSP based receiver implementation for OFDM acoustic modems," *Physical Communication*, vol. 5, no. 1, pp. 22–32, Mar. 2012.

[6] N. Patwari, J. N. Ash, S. Kyperountas, A. O. Hero, R. L. Moses, and N. S. Correal, "Locating the nodes: cooperative localization in wireless sensor networks," *IEEE Signal Process. Mag.*, vol. 22, no. 4, pp. 54–69, Jul. 2005.

[7] H. Tan, R. Diamant, W. Seah, and M. Waldmeyer, "A survey of techniques and challenges in underwater localization," *Ocean Engineering*, vol. 38, no. 14–15, pp. 1663–1676, Oct. 2011.

[8] N. Bilaniu and G.S.K. Wang, "Speed of sound in pure water as a function of temperature," *J. Acoustic Soc. Am.* vol. 93, no 3. pp. 1609 – 1612. Mar. 1993.

[9] Texas Instruments technical references: "Applications Using the TMS320C6000 Enhanced DMA," *SPRA636a*, "TMS320C6000 DSP Software-Programmable Phased-Locked Loop (PLL) Controller Reference Guide," *SPRU233c*, "TMS320C6000 DSP General-Purpose Input/Output (GPIO) Reference Guide,"*SPRU584s*, "TMS320C6000 DSP External Memory Interface (EMIF) Reference Guide,"*SPRU266e*.